

# Optimization of Switched Reluctance Motor for Drive System in Automotive Applications

A. Peniak, J. Makarovič, P. Rafajdus, P. Dúbravka

**Abstract**—The purpose of this work is to optimize a Switched Reluctance Motor (SRM) for an automotive application, specifically for a fully electric car. A new optimization approach is proposed. This unique approach transforms automotive customer requirements into an optimization problem, based on sound knowledge of a SRM theory. The approach combines an analytical and a finite element analysis of the motor to quantify static nonlinear and dynamic performance parameters, as phase currents and motor torque maps, an output power and power losses in order to find the optimal motor as close to the reality as possible, within reasonable time. The new approach yields the optimal motor which is competitive with other types of already proposed motors for automotive applications. This distinctive approach can also be used to optimize other types of electrical motors, when parts specifically related to the SRM are adjusted accordingly.

**Keywords**—Automotive, drive system, electric car, finite element method, hybrid car, optimization, switched reluctance motor.

## I. INTRODUCTION

HYBRIDE or fully electric cars made their entrance to automotive market and have nowadays growing market share. They are increasingly under pressure of price competitiveness with respect to conventional cars. Therefore, each component of the cars is under constant focus of R&D or engineering teams to reach a cost reduction. An electric motor, which is an auxiliary or main part of these cars drive systems, is no exception [1]-[4].

Different types of the electric motors are used to power the cars. Induction motors (IM) [5] and permanent magnet synchronous motors (PMSM) [5], [6] are commonly used. Switched reluctance motors (SRM) [6] are not so common, but can be considered as having a high potential for the cost reduction. However, it is quite a challenge to design SRM that would reach performance parameters of IM or PMSM or even outperform them.

In this field exists several modern methods, which can be used during design process and for its optimization such as Finite Element Method (FEM). Some other methods as genetic algorithms, multi objective design process or particle swarm

This work was supported thanks to Slovak Scientific Grant Agency VEGA No. 1/0940/13.

A. Peniak and P. Dúbravka are with the Department of Power Electrical Systems, University of Žilina, Žilina, 01026 Slovakia (phone: 041 513 2270; e-mail: adrian.peniak@fel.uniza.sk, peter.dubravka@fel.uniza.sk).

J. Makarovič is with the Department of Power Electrical Systems, University of Žilina, Žilina, 01026 Slovakia (phone: 041 513 2274; e-mail: juraj.makarovic@fel.uniza.sk).

P. Rafajdus is with the Department of Power Electrical Systems, University of Žilina, Žilina, 01026 Slovakia (phone: 041 513 2058; e-mail: pavol.rafadus@fel.uniza.sk).

optimization can be used during electrical machine design process, mainly for Switched Reluctance Motor (SRM), [7]-[10].

Our task was to find a way of SRM optimization that would yield SRM fulfilling high customer requirements. The proposed unique optimization, which is described in this paper, is based on an appropriate transformation of

- automotive customer requirements,
- most relevant SRM performance parameters,
- and their underlying independent variables,

to a mathematical description of an optimization problem. Further, the newly proposed optimization algorithm uses synergy between the used software, static and dynamic characteristics of SRM to find an accurate optimal solution within a short period of time.

The optimization starts with an analytical calculation of initial motor dimensions, which are used to set lower and upper limits of design variables [7], [8]. Then, the optimization algorithm continues by creating finite element motor models, from which a set of static motor torque and phase inductance maps are obtained. These maps are further used in dynamic simulations to determine dynamic waveforms of currents, torque and magnetic flux densities in particular parts of the motor. In an inner loop, optimal switching angles are found. The next step is a calculation of output performance parameters that are also objectives that needs to be optimized. The objectives are fed back into the optimization algorithm and the next optimization step is determined. These iterations go on until the optimal solution is found.

In this way, the optimization approach takes into account nonlinearities of the motor, an influence of torque decrease in dynamic state compare to static one and an influence of switching angles.

## II. OPTIMIZATION OF SRM

### A. Automotive Customer Requirements

The customer requirements for the fully electrical driven car are:

- the nominal power of the SRM is 30 kW,
- the power characteristic as a function of revolution should satisfy condition  $P_{2500rpm} \cdot 1.5 \leq P_{5000rpm}$ ,
- the efficiency of the SRM is more than 80% at 5000 rpm,
- the nominal rpm are 5000 rpm,
- the nominal input voltage 500 V,
- the nominal input current 100 A,
- the maximal input current 250 A,
- the maximal outer diameter 250 mm and maximal stack

length of the motor is 300 mm.

### B. Mathematical Formulation of the Optimization Problem

In general, an optimization problem is defined as a set of objective functions, subject to constraints that define the upper and lower bounds of variables. Then, the optimization problem can be written as a system of equations [12]:

$$\text{minimize: } f_m(x), m=1,2,\dots,M \quad (1)$$

$$\text{with constrains: } c_j(x) \leq 0, j=1,2,\dots,J \quad (2)$$

$$\text{and: } c_k(x) \leq 0, j=1,2,\dots,K \quad (3)$$

$$\text{with: } x_i^{(L)} \leq x_i \leq x_i^{(U)} \quad (4)$$

where  $f_m$  is the set of the objective functions,  $c_j$  and  $c_k$  are the set of the equally or the inequally constrains and  $x_i$  is the set of the model dimension variables with lower and upper limits.

In our case, where the customer requirements are known, then the optimization problem can be started as to

$$\text{minimize: } -P_{2500rpm} \quad (5)$$

$$\text{with constrains: } P_{2500rpm} \cdot 1.5 \leq P_{5000rpm} \quad (6)$$

$$\eta \geq 0.8 \quad (7)$$

$$J_{wire} \leq 8 \quad (8)$$

no equality constraints are used,

with: six geometry parameters (see Fig. 1.)  
and the seventh parameter is the number of the winding turns.

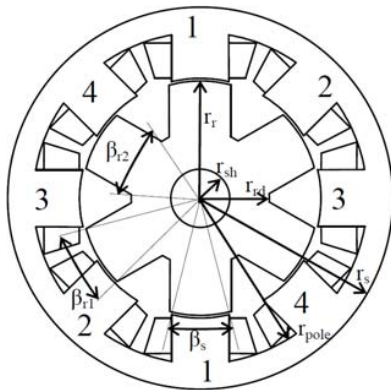


Fig. 1 Cross section area of four phase SRM with set of model dimension variables

The fixed parameters of the motor are:

- the nominal rpm is 5000 rpm,
- the nominal input voltage 500 V,
- the nominal input current 100 A,
- the maximal input current 250 A,
- the maximal outer diameter is 250 mm and the maximal stack length of the motor is 300 mm.

The minimization of the negative motor output ensures the maximization of the power. This definition is selected in order to reach the maximum power density and the minimum use of material and consequently the minimum cost of the motor.

The inequality condition (6) guarantees the power as the function of the revolution to be increasing at least until 5000 rpm.

The minimum required efficiency of the motor is reached by introducing the requirements as the inequality constraint (7).

The inequality constraint (8) is based on experiences. It is the value that creates Joule losses that are possible to cool down by a water cooling system.

The model dimension variables are chosen in order to give the optimization necessary degrees of freedom to allow for sufficient difference between aligned and unaligned phase inductance ( $\approx$  motor torque  $\approx$  output power), but also a change of the phase inductance as function of position. The change of the inductance also gives the possibility to maximize the average value of the motor torque when a phase is switched on.

It is important to mention that the average value of the motor torque is a nonlinear function of the model dimension variables. Therefore, it is possible to find this value analytically only if linearization is applied. However, by the proper choice of the model dimension variables, it is possible to vary the average value of the torque for the optimization purposes. Then, by using the finite element analysis, the accuracy of the calculation does not have to be compromised by a linearization.

The second nonlinearity, which influences the average value of the torque, is a transient behavior of the motor current. Therefore, the dynamic analysis of the motor needs to be a part of the optimization. Consequently, it is also the task of this optimization to find optimal switching angles that maximizes the average value of the torque.

### C. Optimization Algorithm

The proposed algorithm is shown in Fig. 2. The algorithm is based on the static finite element simulations that create torque and phase inductance maps that are utilized by analytical dynamic simulations of the SRM. By this way, the optimization approach takes into account the nonlinearities of the motor, the influence of the torque decrease in the dynamic state compare to static one and the influence of switching angles.

The way, how the optimization works, is described in the following subsections.

#### 1) Analytical Model Calculation

The analytical model calculation program calculates the possible dimensioning of SRM once at the beginning of the optimization. It yields the initial set of the model dimension variables.

These model dimension variables are then used to set their lower and upper limits in order to restrict the variable's space. The limits are then entered in to the Opera optimizer. It results

in a shorter optimization convergence and the total optimization time is significantly reduced.

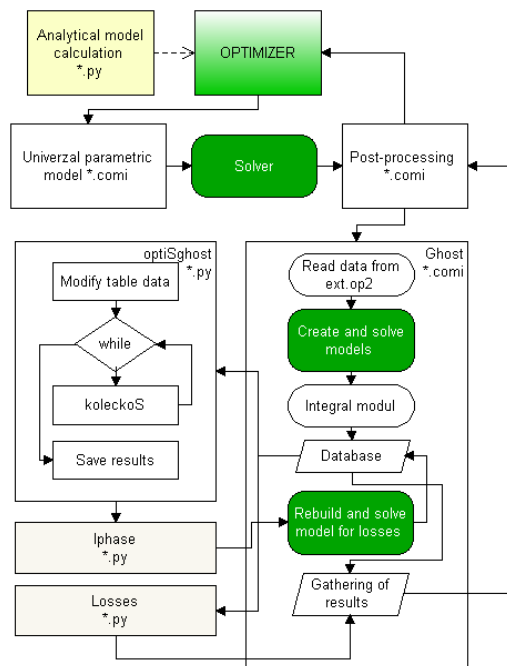


Fig. 2 Block diagram of the proposed optimization algorithm

## 2) Optimizer

The optimizer is standard Opera optimizer software tool that uses a continuous optimization algorithm for multidimensional problems.

## 3) Universal Parametric Geometry model

The universal parametric geometry model is written in Opera command language. It draws geometry of SRM (see Fig. 1). This program is used to draw motor models with new sets of model dimension variables, which are generated by Opera optimizer in each optimization step.

The input data of this file can be divided into two groups, the fixed ones (selected by a designer)

- the number of phases,
- the maximal phase current,
- the number of the stator and the rotor teeth,
- the outer diameter of the motor,
- the diameter of the rotor shaft,
- the air gap,

and the variable ones

- the model dimension variables.

Volume conflicts in the motor could rise from the optimization algorithm, which changes the model dimension variables. To avoid the conflicts a set of scaling rules are defined. The rules are functions of the model dimension variables.

Further, the parametric model defines all materials used in SRM.

The motor model is drawn in polar coordinates. It is then

meshed by using defined mesh lines and arcs parameters of the motor regions.

The SRM model uses a slide air gap region, which is in the middle of other two air gap regions:

- the first is linked to the stator,
- the second is linked to the rotor.

So, the air gap is split in to the three regions. This is given for numerical and mesh generator stability.

## 4) Solver

The Opera static solver is used to solve the motor models created by the universal parametric geometry model program based on the set of model dimension variables generated by Optimizer. The solver is called also in Ghost module.

## 5) Post-Processing

After the solution of the motor model was calculated by the solver, a post-processing module (written in Opera command language) creates an external copy of a related model file, because Opera optimizer do not allow further modifications, which are necessary for our optimization approach. Then, the Post-processing module starts the Ghost module, waits on data from the Ghost and accumulates data for the optimizer.

## 6) Ghost

Ghost module is the heart of our optimization approach, because it creates torque and phase inductance maps.

The torque and phase inductance maps (see Figs. 3 and 4) are actually the torque and the phase inductance as functions of the phase currents and rotor positions in ranges defined by the motor operation limits. These functions are used to map the torque and the phase inductance of the motor needed in the dynamic simulation of the motor behavior in the Optisghost module.

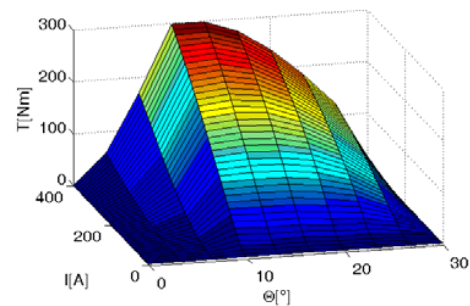


Fig. 3 Motor torque map

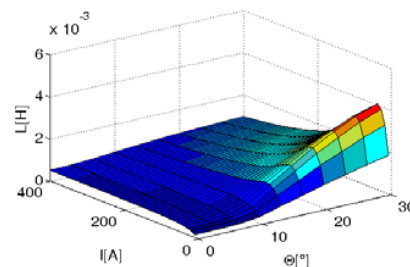


Fig. 4 Phase inductance map

The maps are created as follows. The Ghost reads external copy of the related model file from the Post-processing module, rebuilds the model file to modify the rotor position and the current density in winding regions. Then, it calls Solver to solve in iterations all necessary combinations of the rotor positions and the current densities.

The step of the rotor position depends on the angle from aligned to unaligned position of the rotor tooth. This angle is divided into 11 positions. The step of current density is defined similarly, where the interval from 0A to maximum current is divided into 41 steps.

The output of Ghost is the total torque calculated by using of the command RMTORQUE and the phase inductance is obtained from the magnetic field energy calculated by the integration of the magnetic vector potential and the current density over the current regions in defined positions.

When the maps are completed, Ghost calls OptiSghost module via Linux command and it is waiting for results from the dynamic simulation from OptiSghost.

Integration module is only plug module for Ghost, which opens different motor cases and integrates requested data. Integration module also makes long strings for database, so that the program memory is not overload.

#### 7) OptiSghost

The OptiSghost module is extremely high-speed python program. The main task of OptiSghost is to

- calculate the phase current waveforms,
- obtain the instantaneous torque from the torque map for each corresponding instantaneous phase current,
- integrate the average motor torque from the instantaneous torque,
- calculate the output power at a constant speed,
- optimize the switch ON and the switch OFF angles of the motor phases,

alltasks are included in KoleckoS.

The current waveforms are obtained from a dynamic calculation, where the basic equation that needs to be solved is:

$$di = \frac{\left( v - Ri - i\omega \frac{dL(i, \theta)}{d\theta} \right) dt}{L(i, \theta)} \quad (9)$$

If the current and the rotor position are known, then the static electromagnetic torque can be taken from the torque map:

$$T = fL(i, \theta) \quad (10)$$

The optimization of the switching angles is carried out in each optimization steps, where the dynamic simulation of the motor with different ON and OFF angles is made until the maximum motor torque is found.

OptiSghost can optimize the switch angles in 2.5 minutes, but when it runs in a parallel computing the time reduces to about 16 seconds.

#### 8) Iphase

The Iphase program compiles the phase current of each phase (see Fig. 5.) in to one data file and this file sends back to Ghost. Then, Ghost calls the solver to determine the distribution of the magnetic flux density in the motor.

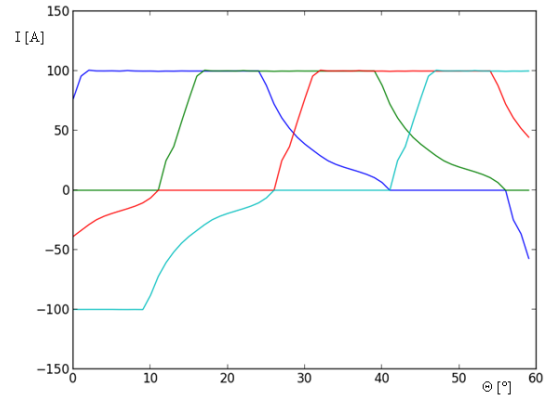


Fig. 5 Four phase currents of the SRM.

#### 9) Losses

The Losses program reads the values of the magnetic flux densities and calculates the average magnetic flux density in defined parts of the motor (see Fig. 6) as a function of the rotor position:

$$B = \frac{\phi}{S} \quad (11)$$

where  $B$  is the average magnetic flux density in defined parts of motor,  $\phi$  is the average magnetic flux in defined parts of motor and  $S$  is cross-section area in defined parts of motor.

Then, the fast Fourier transformation (FFT) is applied to the average magnetic flux densities and based on the modified Steinmetz equation the iron losses are determined [11].

$$f_n = \frac{2\pi \cdot rpm}{60} n \quad (12)$$

$$\Delta P_{Fe} = m \sum_{i=0}^{50} \left( k_h \frac{f_n}{50} B^2 + k_v \left( \frac{f_n}{50} \right)^2 B^2 \right) \quad (13)$$

where  $m$  is the mass in defined parts of motor,  $n$  is the harmonic order and the coefficients are chosen  $k_v=1.6$  and  $k_h=1.1$  based on the core material.

The Joule losses in the coils are calculated by Ohm's law:

$$\Delta P_{Cu} = \sum_{i=0}^{50} R_n I_n^2 \quad (14)$$

where  $R$  is the phase resistance and  $I$  is the rms value of the current of  $n$  harmonic order.

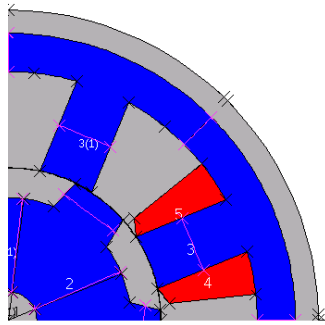


Fig. 6 Defined parts of the motor (in pink) for calculation of the average magnetic flux densities

### III. RESULTS

#### A. Optimized SRM

The optimized motor (see Fig. 7 (a)) is obtained by the described optimization approach, which starts from the initial motor geometry (see Fig. 7 (b)).

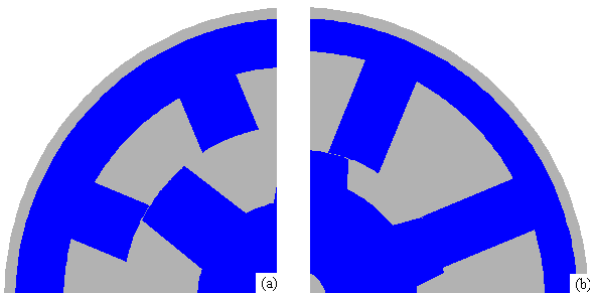


Fig. 7 The optimized (a) and initial (b) motor geometry

From Fig. 7 several differences can be seen. The optimized motor compare to the initial one has

- significantly higher rotor teeth,
- the radius of the air gap is larger,
- the height of the stator yoke is increased,
- the height of the rotor yokes is decreased,
- the cross section of the stator winding is reduced,
- and the number of the coil turns is changed from 20 to 30 turns.

The motor stack length and the outer diameter of the both motors stayed the same 150 mm and 250 mm, respectively.

#### B. Torque and Current Waveforms

The motor torques and the currents from the dynamic simulation of the initial and the optimized motors are shown in Figs. 8 and 9.

It can be seen, that the optimized motor has the peak torque of one phase around 97 Nm compare to 70 Nm of the initial motor.

The rest of the calculated performance parameters also show improvements of the optimized motor with respect to the initial one (see Table I).

The motor torques and the output power from the dynamic simulation of the optimized motors are shown in Fig. 10. It

can be seen, that the optimized motor has the maximal output power 70 kW around 18000 rpm.

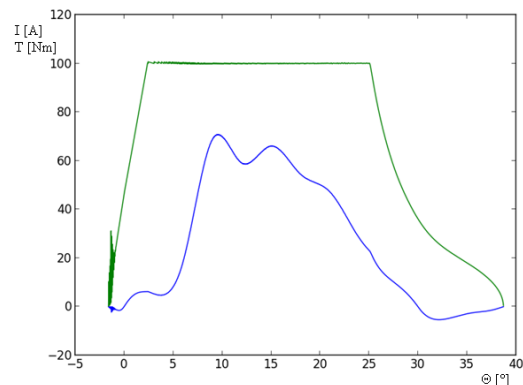


Fig. 8 The phase current waveform (green) and the torque of one phase (blue) of the initial motor.

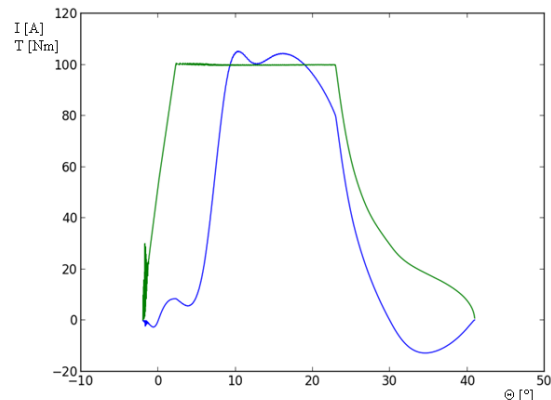


Fig. 9 The phase current waveform (green) and the torque of one phase (blue) of the optimal motor.

TABLE I  
PERFORMANCE PARAMETERS OF THE INITIAL AND OPTIMIZED MOTORS AT 5000RPM AND 100A

Type of motor	$P_{out}$ [kW]	$\eta$ [%]	Power density [kW/l]	Switch ON [°]	Switch OFF [°]	Average torque [Nm]
Initial motor	21.8	78.8	2.96	-1.6	22.5	41.6
Optimized motor	46.0	88.1	6.247	-2.0	22.9	87.8

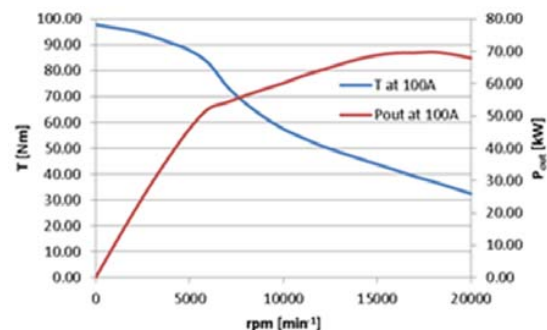


Fig. 10 The motor torque and the output power as the function of the speed of the optimal motor

*C. Losses*

The iron losses are calculated from harmonic components of the average magnetic flux densities (see Figs. 11-16).

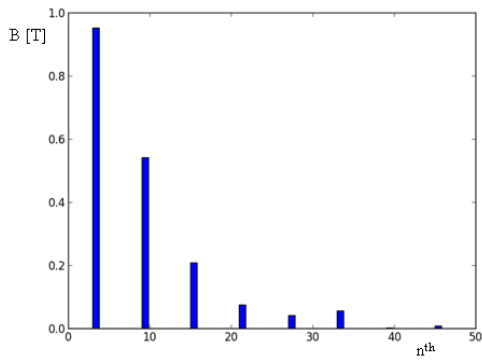


Fig. 11 FFT of the average magnetic flux density in stator teeth of the initial motor

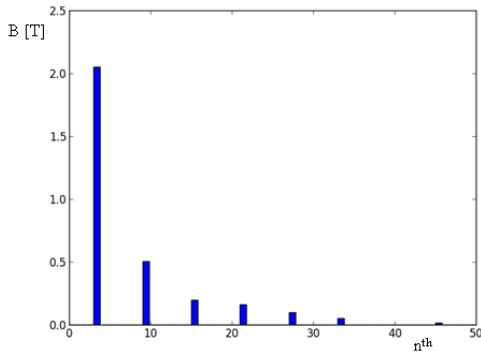


Fig. 12 FFT of the average magnetic flux density in stator yoke of the initial motor

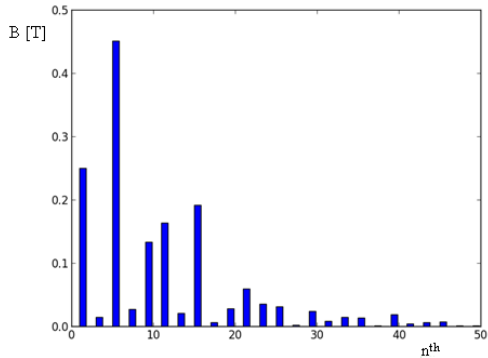


Fig. 13 FFT of the average magnetic flux density in rotor teeth of the initial motor

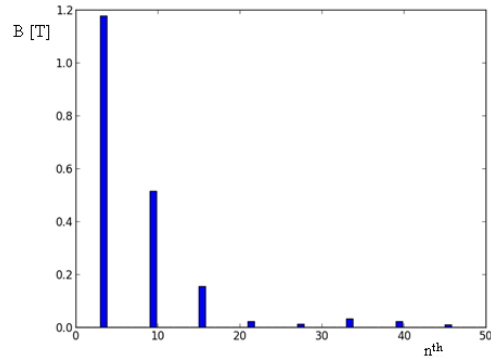


Fig. 14 FFT of the average magnetic flux density in stator teeth of the optimized motor

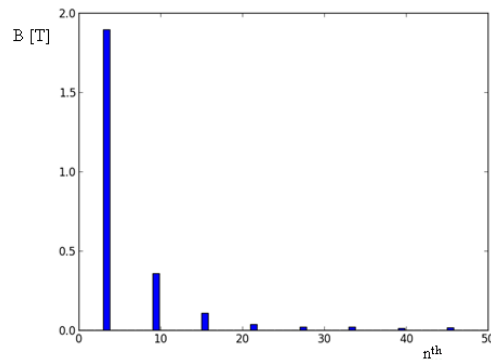


Fig. 15 FFT of the average magnetic flux density in stator yoke of the optimized motor

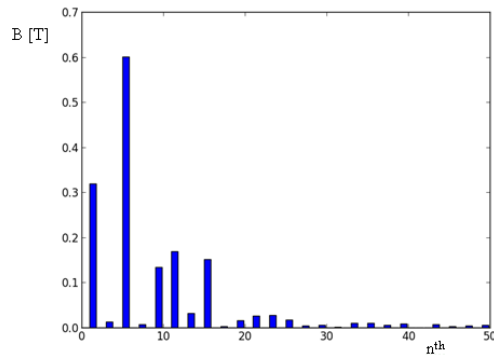


Fig. 16 FFT of the average magnetic flux density in rotor teeth of the optimized motor

When comparing the main harmonic of different parts of the optimized motor, the average magnetic flux density is more evenly distributed than in the initial motor and does not exceed 1.9 T. The optimized SRM has a comparable magnetic flux density and lower spectrum of harmonics than the initial motor.

The obtained losses in determined parts of the motor are listed in Table II.

TABLE II  
LOSSES IN PARTS OF INITIAL AND OPTIMIZED MOTOR AT 5000RPM AND 100A

Type of motor	$P_{Cu}$ [W]	$P_{stator\ teeth}$ [W]	$P_{stator\ yoke}$ [W]	$P_{rotor\ teeth}$ [W]	$P_{rotor\ yoke}$ [W]
Initial motor	517.2	1696.0	3900	194.9	263.3
Optimized motor	1278.2	978.1	3162.7	529.9	306.4

The losses of the optimized motor are in a range from 306 W to 3163 W, whereas the range of the initial motor losses is from 195 W to 3900 W.

The total losses of the optimal and the initial motor are 6255.3 W and 4875.4 W, respectively.

#### IV. DISCUSSION

Based on the results, the initial geometry of the motor undergoes several changes during the optimization process. The first, the optimization process tries to increase the power of the motor by the increase of the motor torque through the increase of the rotor saliency. The second, the motor torque is increased by the enlarged radius of the air gap.

The optimal motor geometry is further influenced also by the inequality condition of the efficiency that causes more even space distribution of the average magnetic flux densities and lower values of the overall maximum of the magnetic field density.

In the iron parts of the motor, a higher harmonic content of the magnetic flux densities are also visible. The stator harmonics of the magnetic flux densities are caused by shape of the coils currents. While, the rotor magnetic flux densities contain also harmonics caused by an interference of the stator and the rotor teeth saliency.

The iron losses of the optimal motor have a similar pattern as the magnetic flux density that is narrower spread over the different parts of the motor. Although, the optimized motor has higher losses, its efficiency is higher due to the higher output power.

The performance parameter of the optimized SRM that is outstanding compare to other SRMs is the volumetric power. The volumetric power is almost double compare to conventional SRMs [5].

The optimized SRM is compared with IPMSM in Table III. It can be seen that the optimized motor outperforms the IPMSMs.

TABLE III  
COMPARISON SELECTED PARAMETERS OF OPTIMIZED SRM AND IPMSM

Selected parameter	The optimized motor	2 <sup>nd</sup> generation IPMSM [6]	3 <sup>rd</sup> generation IPMSM[6]
Outer diameter of stator	250 mm	269 mm	264 mm
Motor axial length	150 mm	156 mm	108 mm
Max output power	70 kW	50 kW	60 kW
Maximal torque	98/249.5** Nm	400 Nm	207 Nm
DC side voltage	500V	500V	650V
Current RMS	100/250** A	169 A	141 A
Current density	7.6 A/mm <sup>2</sup>	18 A/mm <sup>2</sup>	19 A/mm <sup>2</sup>
$\eta$	92%*	85%*	91%*
Volumetric power	9.48 kW/l	5.6 kW/l	10,2kW

\*estimated, \*\*18 sec overload

It can be said that the optimization approach gives results as expected, because the output power according the objective function is reached. The output power of SRM is reached with high margin, even though the outer dimensions were chosen based on the IPMSM of the second generation.

#### V. CONCLUSION

To conclude, the proposed optimization method is able to optimize SRM within 72 h, so the motor reaches the parameters of currently used IM and SMPM and outperforms in several attributes other SRMs.

Because the optimization yields SRM with higher performance than required, the objective function and the constraints can be reformulated so that the optimized SRM will be closer to the requirements as for example

- minimize  $-\eta$
- $30\text{kW} < P_{5000} < 35\text{kW}$
- $P_{4900} < P_{5000}$
- add the effective length of the motor as the model dimension.

This unique approach can also be used to optimize other types of the motors, when parts specifically related to switched reluctance motor are adjusted accordingly.

#### REFERENCES

- [1] K.M. Rahman, B. Fahimi, G. Suresh, A.V. Rajarathnam, M. Ehsani: *Advantages of switched reluctance motor applications to EV and HEV: design and control issues*, IEEE Transactions on Industry Applications, vol. 36, no. 1 (January-February 2000), pp. 111-121.
- [2] C. Kamalakannan, V. Kamaraj, S. Paramasivam, S. Paranjothi: *Switched reluctance machine in automotive applications – A technology status review*, in Proceedings of the 1st International Conference on Electrical Energy Systems (ICEES '2011), Newport Beach (CA, USA), 2011, pp. 187-197.
- [3] M. Krishnamurthy, C.S. Edrington, A. Emadi, P. Asadi, M. Ehsani, B. Fahimi: *Making the case for applications of switched reluctance motor technology in automotive products*, IEEE Transactions on Power Electronics, vol. 21, pp. 659-675, 2006.
- [4] I. Nuca, P. Todos, V. Eşanu: *Urban electric vehicles traction: Achievements and trends*, in Proceedings of the International Conference and Exposition on Electrical and Power Engineering (EPE '2012), Iaşi (Romania), pp. 76 81, 2012.
- [5] A. Emadi: *Handbook of Automotive Power Electronics and Motor Drivers*, Taylor and Francis New York 2005, ISBN: 978-0-824-72361-3.
- [6] K. Kiyota, A. Chiba: *Energy Conversion Congress and Exposition (ECCE)*, 2011 IEEE, pp. 3562-3567.
- [7] J. Pyrhonen, T. Jokinen, V. Hrabovcová: *Design of Rotating Electrical Machines*, John Wiley&Sons Ltd., Chichester, West Sussex, United Kingdom, 2008, ISBN: 978-0-470-69516-6
- [8] Miller, T. J. E.: *Electronic Control of Switched Reluctance Machines*, Oxford (U.K.): Newnes, 2001.
- [9] JieGao, Hexu Sun, Lin He, Yan Dong, Yi Zheng: *Optimization Design of Switched Reluctance Motor based on Particle Swarm Optimization*, in Electrical Machines and Systems (ICEMS), 2011 International Conference on, 2011, pp. 1-5.
- [10] Xue, X.D., Cheng, K.W.E., Ng, T.W., Cheung, N.C.: *Multi-Objective Optimization Design of In-Wheel Switched Reluctance Motors in Electric Vehicles*, IEEE Transactions on Industrial Electronics, vol. 57, no. 9, september 2010, pp. 2980 - 2987.
- [11] P. Rafajdus, V. Hrabovcová, P. Hudak, "Investigation of Losses and Efficiency in Switched Reluctance Motor", in Proceedings of the 12th International Power Electronics and Motion Control Conference (EPE PEMC '2006), Portoroz (Slovenia), 2006.
- [12] Opera 14R1 manual

**Adrian Peniak** (M'14) was born in Banská Bystrica, Slovakia in 1988. He became a Member (M) of IEEE in 2014. He graduated and obtained his M.Sc. in field Electroenergetics, at University of Žilina, Slovakia in 2013. Currently, he is a PhD. student at department of power electronic systems (University of Žilina) dealing with a design of an electrical motors for automotive applications.

During his M.Sc. study, he started to participate on APVV project dealing with diagnostics of power Transformers. He was also involved in optimization of ASM for compressors in Product development department in Secop s.r.o. Zlaté Moravce.

**Juraj Makarovič** was born in Košice, Slovakia in 1974. He graduated and obtained his M.Sc. in field of electrical traction, at University of Žilina, Slovakia in 1997. Then, he obtained his MTD. in field of mechatronics and PhD. in electromechanics at Technical University in Eindhoven, The Netherlands, in 2001 and 2006, respectively.

He continued as an External consultant at ASML B.V. The Netherlands, a Project leader at EVPU a.s. Slovakia, he also worked as Product development director in Secop s.r.o., Slovakia. Currently, he is a Scientific researcher in field of electrical drives for automotive at University of Žilina, Slovakia.

**P. Rafajdus** (M'08-SM'12) was born in Trnava, Slovakia, in 1971. He received the M.Sc. degree in electrical engineering and the Ph.D. degree from the University of Žilina, Žilina, Slovakia, in 1995 and 2002, respectively. Currently, he is an Associate Professor at the Faculty of Electrical Engineering, University of Žilina. His research is focused on the electrical machines, mainly switched reluctance motors, and other electrical machine properties.

Hrabovcová, V., Rafajdus, P., Franko, M., Hudák, P.: *Testing and Modeling of Electrical Machines*, publisher EDIS University of Žilina, Slovakia, Žilina, second edition, 2009, p.: 335, in slovak language,

Hrabovcová, V., Rafajdus, P.: *Electrical Machines. Theory and Examples*, publisher EDIS University of Žilina, Slovakia, Žilina, 2009, p.: 415, in slovak language, ISBN 978-80-554-0101-0

Hrabovcová, V.; Janoušek, L.; Rafajdus, P.; Ličko, M.: *Modern electrical machines*, publisher EDIS University of Žilina, Slovakia, Žilina, 2001, p.: 265, ISBN 80-7100-809-5

**Peter Dúbravka** was born in Považská Bystrica, Slovakia in 1988. He received M.Sc. degree, in field Electric Drives, at University of Žilina, Slovakia in 2012. He is currently a PhD student at the same university. His research interests include electrical machines and drives, control of variable electric drives, fault diagnosis and fault tolerant control. Currently, he is mainly focused on the analysis and development of fault tolerant control techniques for switched reluctance motor drives.